

REPORT

## c-Myc is a novel target of cell cycle arrest by honokiol in prostate cancer cells

Eun-Ryeong Hahm<sup>a,b</sup>, Krishna Beer Singh<sup>a,b</sup>, and Shivendra V. Singh<sup>a,b</sup>

<sup>a</sup>Department of Pharmacology & Chemical Biology, University of Pittsburgh School of Medicine, Pittsburgh, Pennsylvania, USA; <sup>b</sup>University of Pittsburgh Cancer Institute, University of Pittsburgh School of Medicine, Pittsburgh, Pennsylvania, USA

### ABSTRACT

Honokiol (HNK), a highly promising phytochemical derived from *Magnolia officinalis* plant, exhibits *in vitro* and *in vivo* anticancer activity against prostate cancer but the underlying mechanism is not fully clear. This study was undertaken to delineate the role of c-Myc in anticancer effects of HNK. Exposure of prostate cancer cells to plasma achievable doses of HNK resulted in a marked decrease in levels of total and/or phosphorylated c-Myc protein as well as its mRNA expression. We also observed suppression of c-Myc protein in PC-3 xenografts upon oral HNK administration. Stable overexpression of c-Myc in PC-3 and 22Rv1 cells conferred significant protection against HNK-mediated growth inhibition and G<sub>0</sub>-G<sub>1</sub> phase cell cycle arrest. HNK treatment decreased expression of c-Myc downstream targets including Cyclin D1 and Enhancer of Zeste Homolog 2 (EZH2), and these effects were partially restored upon c-Myc overexpression. In addition, PC-3 and DU145 cells with stable knockdown of EZH2 were relatively more sensitive to growth inhibition by HNK compared with control cells. Finally, androgen receptor overexpression abrogated HNK-mediated downregulation of c-Myc and its targets particularly EZH2. The present study indicates that c-Myc, which is often overexpressed in early and late stages of human prostate cancer, is a novel target of prostate cancer growth inhibition by HNK.

### ARTICLE HISTORY

Received 11 March 2016  
Revised 7 June 2016  
Accepted 8 June 2016

### KEYWORDS

androgen receptor; chemoprevention; c-Myc; EZH2; honokiol; prostate cancer

### Introduction

In spite of tremendous advances in our understanding of the prostate cancer biology and underlying risk factors, this malignancy is the cause of thousands of deaths every year in the United States.<sup>1–4</sup> For example, >27,000 American men are expected to die from prostate cancer in 2015 according to the projections from the American Cancer Society. Plants used in alternative and complimentary medicine are attractive for identification of small molecules potentially useful for prevention and/or treatment of prostate cancer.<sup>5</sup> *Magnolia* tree is one such example whose bark extract is widely used in the traditional medicine practices in China, Korea, and Japan.<sup>6</sup> The bioactive lignans in the bark, seed cones, and leaves of *Magnolia* tree include honokiol (HNK), magnolol, and obovatol but former is the best characterized for its anticancer activity.<sup>7,8</sup> Anticancer effects of *Magnolia* lignans, including HNK, were initially studied in human leukemia cell lines.<sup>9</sup> Bai et al.<sup>10</sup> were the first to provide *in vivo* evidence for anticancer activity of HNK in angiosarcoma. *In vivo* tumor growth inhibitory effect of HNK was subsequently extended to solid tumor models, including colorectal,<sup>11</sup> prostate,<sup>12</sup> breast,<sup>13</sup> and brain<sup>14</sup> tumors. HNK or its liposomal preparation was also shown to inhibit metastasis *in vivo* in different preclinical models.<sup>12,15,16</sup> More recent studies have demonstrated cancer chemopreventive activity for this interesting phytochemical.<sup>17,18</sup> For example, HNK administration significantly decreased *N*-nitroso-trischloroethylurea-induced lung squamous cell carcinoma development in mice.<sup>18</sup>

Other intriguing anticancer properties of HNK include inhibition of epithelial to mesenchymal transition providing mechanistic explanation for its anti-metastatic activity and cancer stem cells.<sup>12,15,19,20</sup> Furthermore, liposomal HNK was shown to sensitize cancer cells to drugs such as cisplatin.<sup>21</sup> In summary, preclinical evidence for anticancer effect of HNK is quite persuasive.

Our laboratory was the first to demonstrate *in vivo* anticancer activity of HNK after oral administration using an androgen-independent human prostate cancer (PC-3) xenograft model.<sup>22</sup> Specifically, gavage with 2 mg HNK/mouse, 3 times/week, significantly retarded growth of PC-3 cells subcutaneously implanted in male nude mice.<sup>22</sup> At the cellular level, HNK-treated prostate cancer cells (PC-3 and LNCaP) exhibited G<sub>0</sub>-G<sub>1</sub> phase cell cycle arrest that was associated with suppression of total and phosphorylated retinoblastoma protein and inhibition of E2F1 transcriptional activity.<sup>23</sup> Even though HNK treatment resulted in induction of cell cycle inhibitor p21 (PC-3 and LNCaP) as well as tumor suppressor p53 (LNCaP), silencing of these proteins did not impact cell cycle arrest by HNK treatment.<sup>23</sup> HNK-induced apoptosis in prostate cancer cells was accompanied by induction of Bax and Bak, and their silencing conferred partial yet significant protection against cell death induction.<sup>22</sup>

More recent studies from our laboratory have shown inhibition of androgen receptor (AR) expression and activity (e.g., decrease in prostate-specific antigen expression and secretion)

by HNK and its synthetic dichloroacetate analog in prostate cancer cells.<sup>24</sup> Because *c-Myc* is a ligand-independent transcriptional target of AR,<sup>25</sup> the present study was logically designed to determine the role of *c-Myc* in anticancer effects of HNK.

## Results

### **HNK treatment decreased *c-Myc* protein level in prostate cancer cells**

We showed previously that PC-3 (an androgen-independent cell line lacking AR expression) and LNCaP cells (an androgen-responsive cell line expressing T877A mutant of AR) are sensitive to growth inhibition by HNK (chemical structure of HNK is shown in Fig. 1A) at pharmacological doses.<sup>14,23,26</sup> The present study extended these findings by demonstrating dose-dependent cell viability inhibition by HNK in additional human prostate cancer cell lines, including 22Rv1 (a castration-resistant prostate cancer cell line with expression of AR splice variants) and VCaP cells (a prostate cancer cell line with wild-type AR expression), and Myc-CaP cell line derived from prostate tumor of a transgenic mouse<sup>27</sup> (Fig. 1B). Western blot data for the effect of HNK treatment on total *c-Myc* protein level in human prostate cancer cells are shown in Figure 1C. HNK-mediated downregulation of *c-Myc* protein was apparent even at 8 hour time point in most cells (Fig. 1C). Near complete loss of *c-Myc* protein 24 hour post-HNK exposure was clearly evident in highly aggressive C4-2 and 22Rv1 cells (Fig. 1C). Similarly, HNK treatment decreased *c-Myc* protein level in murine prostate cancer cell line Myc-CaP (Fig. 1D). These results indicated downregulation of *c-Myc* protein after HNK treatment in a panel of human and mouse prostate cancer cell lines.

### **HNK treatment decreased nuclear levels of *c-Myc***

Previous immunohistochemical studies using tissue microarrays have shown that nuclear *c-Myc* protein overexpression is frequent in prostatic intraepithelial neoplasia as well as in primary and metastatic adenocarcinoma.<sup>28</sup> We therefore explored the possibility of whether nuclear level of *c-Myc* protein was decreased by HNK treatment in cultured cells (Fig. 2A) and xenografted tumors (Fig. 2B). Expression of *c-Myc* protein was mainly confined to the nucleus in every prostate cancer cell line studied in the present study (Fig. 2A). In each cell line, HNK treatment dose-dependently decreased nuclear levels of *c-Myc* protein (Fig. 2A). Furthermore, nuclear staining for *c-Myc* protein was lower by 43–50% in PC-3 xenografts from HNK-treated mice in comparison with control (Fig. 2C). However, the difference was not significant due to large data scatter and small sample size. Nevertheless, these results showed inhibition of nuclear levels of *c-Myc* after HNK treatment in prostate cancer cells *in vitro* and *in vivo*.

### **Effect of HNK treatment on *c-Myc* phosphorylation in human prostate cancer cells**

The *c-Myc* expression is also controlled by sequential phosphorylation at S62 and T58.<sup>29</sup> The S62 phosphorylation contributes to the stability of *c-Myc* protein while phosphorylation

at T58 facilitates its degradation.<sup>29</sup> To gain insights into the mechanism underlying *c-Myc* protein downregulation in HNK-treated cells, initially we examined *c-Myc* phosphorylation. Cell line-specific differences in S62 (Fig. 3A) and T58 (Fig. 3B) phosphorylation following 24 hour HNK treatment were evident in most cell lines. For example, S62 phosphorylation of *c-Myc* was decreased in the PC-3 (null p53), 22Rv1 (mutant p53), and VCaP (mutant p53) cells at least after 24 hour HNK treatment but this was not the case in the LNCaP and C4-2 cells that express wild-type p53. In these cell lines, HNK treatment instead resulted in an increase in p62 phosphorylated *c-Myc*. The possibility that cell line-specific differences are partly related to p53 status requires further investigation. Because a clear-cut pattern did not emerge with respect to the effect of HNK on phosphorylation of *c-Myc*, it is difficult to conclude whether stability of the *c-Myc* protein is affected by HNK treatment.

### **HNK treatment downregulated *c-Myc* mRNA in prostate cancer cells**

Because effect of HNK on *c-Myc* phosphorylation was not conclusive, we attempted to examine whether HNK affects the mRNA expression of *c-Myc*. As seen in Figure 4A and B, exposure of LNCaP and C4-2 cells to 40  $\mu$ M of HNK resulted in downregulation of *c-Myc* at 16 and 24 hour time points in both cell lines. Data for lower dose of HNK were inconsistent (results not shown). HNK-mediated reduction of *c-Myc* protein (Fig. 1C) and its mRNA (Fig. 4A and B) was observed but the effect was more pronounced on the protein level. This can be possibly explained by the involvement of p53 in *c-Myc* downregulation in HNK-treated LNCaP and C4-2 cells. A study from Sachdeva *et al.*<sup>30</sup> demonstrated that p53 represses *c-Myc* expression via induction of miR-145 which directly targets *c-Myc*. We have found that HNK is an inducer of p53 expression in LNCaP cells.<sup>23</sup> Therefore, p53 induction following HNK exposure can augment its inhibitory effect on *c-Myc* in LNCaP and C4-2 cells. However, further work is needed to systematically explore this possibility. Because *c-Myc* functions as a transcription factor and HNK greatly diminished its nuclear level as shown in Figure 2A, it was of interest to check if the transcriptional activity of *c-Myc* was inhibited by HNK treatment. As seen in Figure 4C and D, HNK (24 hour treatment) repressed the *c-Myc* transcriptional activity dose-dependently in both LNCaP and C4-2 cells. Collectively, *c-Myc* downregulation in LNCaP and C4-2 cells by HNK treatment can be explained due in part to repression of its transcription.

### **Functional significance of *c-Myc* downregulation by HNK**

We stably overexpressed *c-Myc* protein in both PC-3 and 22Rv1 cells (abbreviated as Myc\_PC-3 or Myc\_22Rv1, respectively) to study its role in anticancer effects of HNK. Overexpression of *c-Myc* was confirmed by immunoblotting (Fig. 5A). Colony formation assay revealed dose-dependent inhibition after HNK treatment in PC-3 and 22Rv1 cells stably transfected with the empty vector (abbreviated as EV\_PC-3 or EV\_22Rv1,

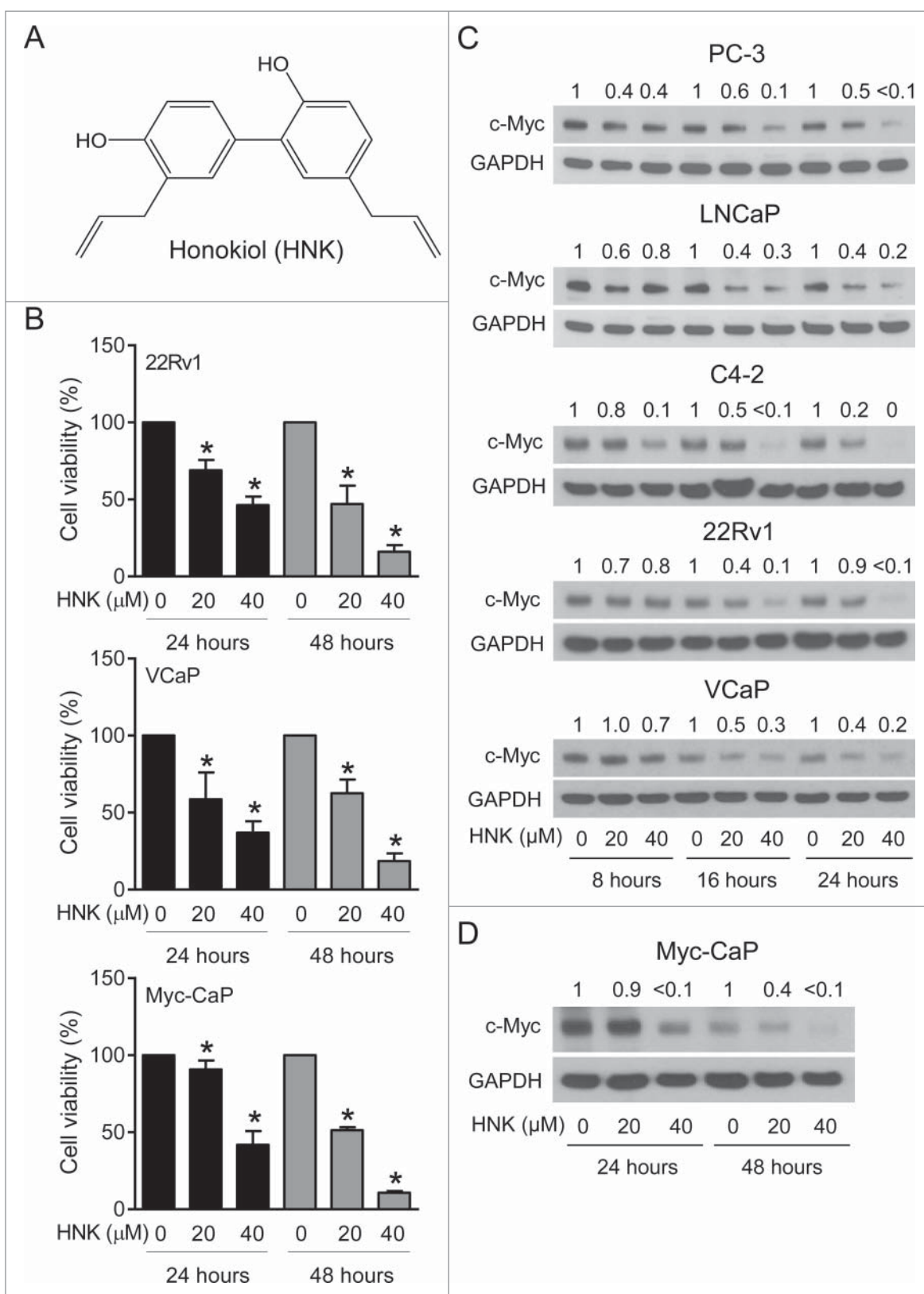


**Figure 1.** HNK treatment decreases c-Myc protein level in prostate cancer cells. (A) Chemical structure of HNK. (B) Viability of 22Rv1 and VCaP human prostate cancer cells and Myc-CaP mouse prostate cancer cells after 24 hour or 48 hour treatment with DMSO or the indicated doses of HNK. Combined results from 2 independent experiments are shown as mean  $\pm$  SD ( $n = 6$ ). Statistical significance compared with respective DMSO-treated control was determined by one-way ANOVA with Dunnett's adjustment (\*,  $P < 0.05$ ). (C) Western blots for total c-Myc and GAPDH using lysates from cells treated with DMSO or the indicated doses of HNK. Numbers on top of the bands are fold changes in protein levels relative to respective DMSO-treated control. (D) Western blots for total c-Myc and GAPDH using lysates from Myc-CaP cells treated with DMSO or indicated doses of HNK. The results were consistent in 2 independent experiments.



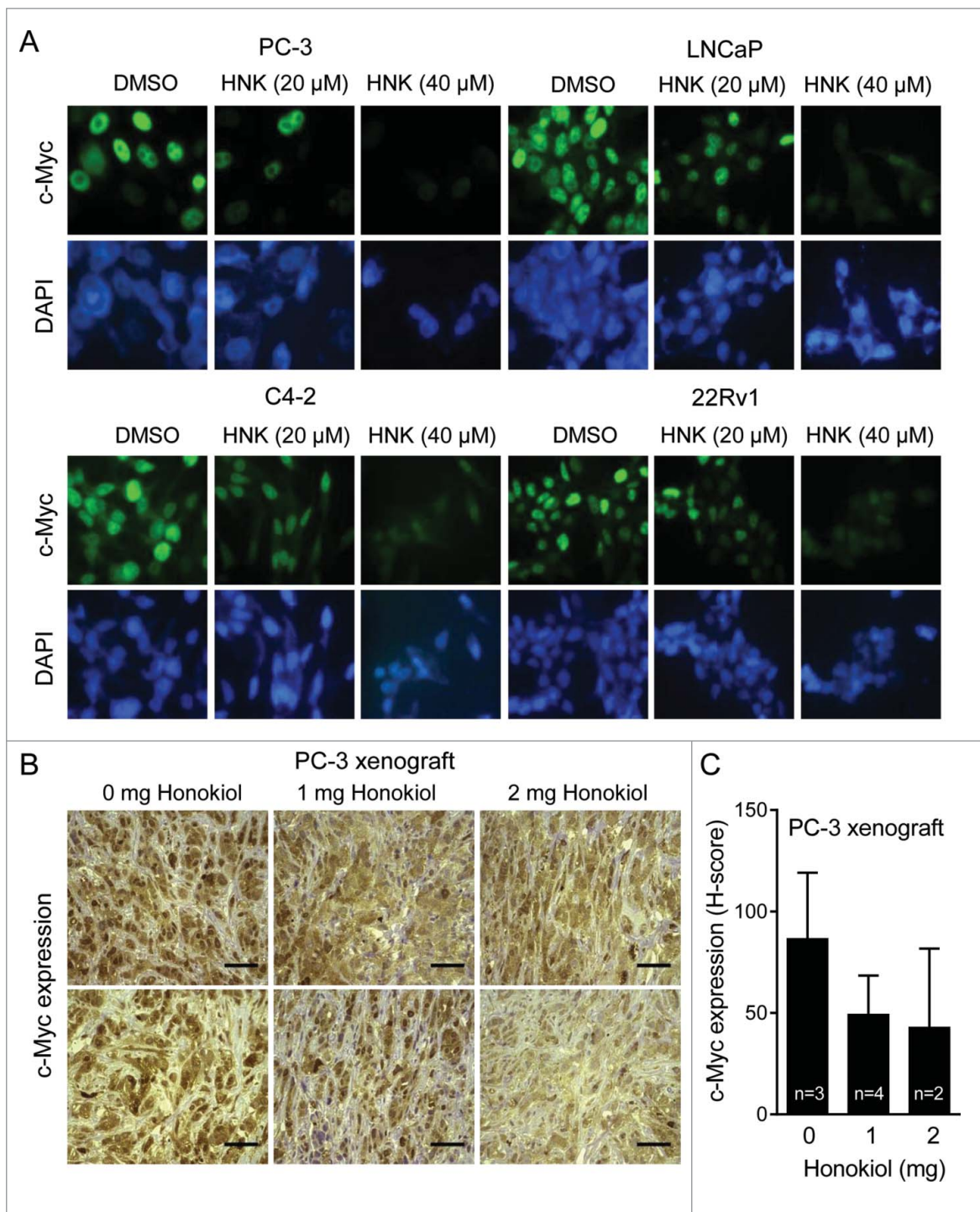


**Figure 2.** HNK treatment inhibits nuclear levels of c-Myc protein in prostate cancer cells. (A) Representative images for c-Myc protein levels in PC-3, LNCaP, C4-2, and 22Rv1 human prostate cancer cells after 24 hour treatment with DMSO or the indicated doses of HNK. (B) Representative images for c-Myc protein expression in tumor sections from PC-3 xenografts. Magnification, 400  $\times$ ; Scale bars = 100  $\mu$ m. (C) Quantitation of c-Myc protein expression in PC-3 xenograft. Results shown are mean  $\pm$  SD.

respectively) (Fig. 5A and 5B). Overexpression of c-Myc increased the number of colonies compared to corresponding empty vector transfected cells. Notably, HNK-mediated inhibition of colony formation was significantly attenuated by c-Myc overexpression and this protection was quite obvious at the highest dose (Fig. 5B). For example, colony formation was reduced by >90% in both EV\_PC-3 and EV\_22Rv1 cells after treatment with 20  $\mu$ M HNK. Under similar treatment

conditions, inhibition of colony formation was only about 46% in Myc\_PC-3 cells and 38% in Myc\_22Rv1 cells (Fig. 5B).

We have shown previously that HNK treatment results in G<sub>0</sub>-G<sub>1</sub> cell cycle arrest.<sup>23</sup> Figure 5C depicts flow histograms for cell cycle distribution in EV\_PC-3, Myc\_PC-3, EV\_22Rv1, and Myc\_22Rv1 cells after 16 hour treatment with dimethyl sulfoxide (DMSO) or HNK. The HNK-mediated cell cycle arrest was also significantly attenuated in c-Myc overexpressing cells

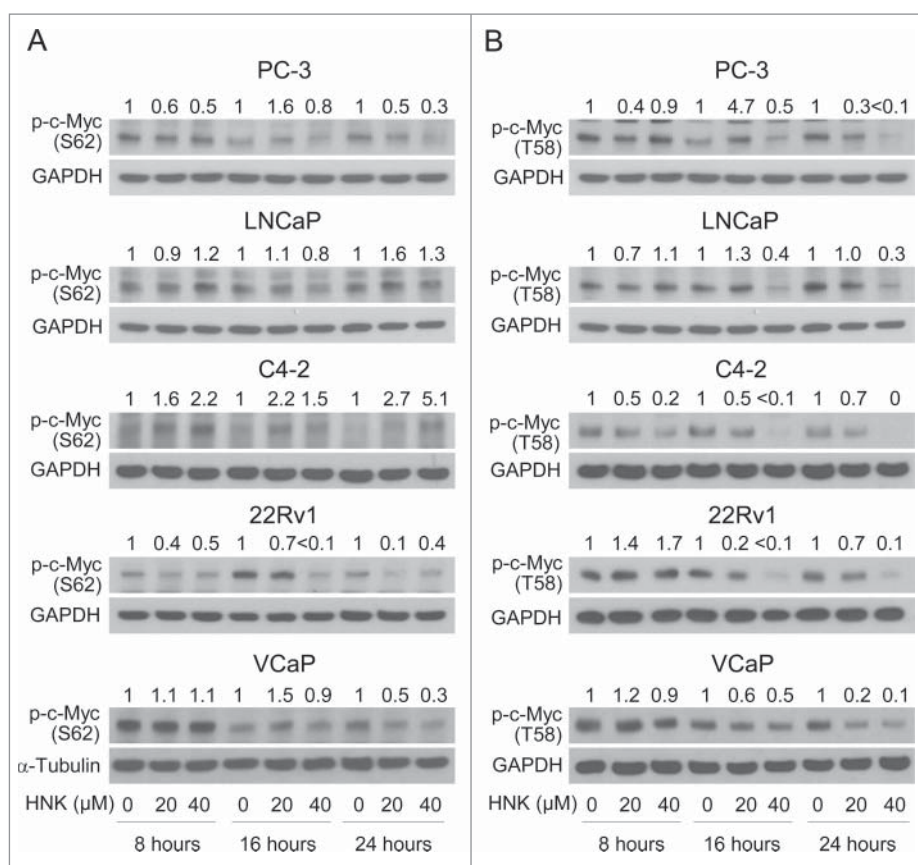


**Figure 3.** Effect of HNK treatment on phosphorylation of c-Myc. Western blots for S62-phosphorylated (A) and T58-phosphorylated (B) c-Myc using lysates from prostate cancer cells following treatment with DMSO or the indicated doses of HNK. Numbers on top of bands represent fold changes in protein levels relative to respective DMSO-treated control.

(Fig. 5D). Based on these results, it is logical to conclude that growth inhibitory effects of HNK in prostate cancer cells are mediated at least in part by c-Myc downregulation.

The HNK-mediated cell cycle arrest in prostate cancer cells is accompanied by downregulation of Cyclin D1, which is a target of c-Myc.<sup>23,31</sup> Because cell cycle arrest by HNK was significantly attenuated by c-Myc overexpression (Fig. 5D), we proceeded to determine protein expression of Cyclin D1 and another c-Myc target (Enhancer of Zeste Homolog 2; EZH2)<sup>32</sup> in c-Myc overexpressing cells after treatment with DMSO or HNK (Fig. 6A). HNK treatment decreased the expression of Cyclin D1 and EZH2 in EV\_PC-3 and EV\_22Rv1 cells (Fig. 6A). Moreover, expression of both proteins was increased in c-Myc overexpressing cells as expected (Fig. 6A). In addition, c-Myc overexpression conferred partial but marked protection against HNK-mediated downregulation of Cyclin D1 and EZH2 at least at the 20  $\mu$ M concentration in both cell lines (Fig. 6A). This protection was also evident at the highest dose in the 22Rv1 cells (Fig. 6A).

#### Effect of AR overexpression on HNK-mediated downregulation of c-Myc

Next, we determined the role of AR in c-Myc downregulation by HNK. Immunoblotting for green fluorescent protein (GFP) confirmed overexpression of AR in stable GFP-tagged AR overexpressing (GFP-AR\_PC-3) cells (Fig. 6B). Consistent with the

data shown in Figure 6A, HNK treatment dose-dependently decreased protein levels of c-Myc and its targets Cyclin D1 and EZH2 in stable GFP-tagged empty vector transfected GFP-EV\_PC-3 cells (Fig. 6B). The HNK-mediated downregulation of all these proteins was partially or fully reversed by AR overexpression. Moreover, stable knockdown of EZH2 resulted in sensitization of PC-3 and DU145 cells to HNK (Fig. 6C and D). Together, these results clearly indicated that AR overexpression confers protection against c-Myc downregulation by HNK.

#### Discussion

Literature data indicate that c-Myc is a valid target for prevention and treatment of human prostate cancer. Overexpression of c-Myc, which plays an important role in cellular metabolism and proliferation, was shown to induce prostatic intraepithelial neoplasia in association with Nkx3.1 loss in a murine model.<sup>33-35</sup> The c-Myc oncogene is often amplified in metastatic prostate cancer and nuclear Myc overexpression seems to be an early event in prostate carcinogenesis.<sup>28,34,36</sup> Moreover, molecular similarities have been observed in Myc-driven prostate cancer in a mouse model and human disease.<sup>37,38</sup> The present study reveals that c-Myc is a functionally important molecular target in anticancer effect of HNK. The c-Myc downregulation by HNK is apparent in a panel of human prostate cancer cells differing in AR mutational status and AR splice variant expression, androgen sensitivity, and p53 expression. The *in vitro*

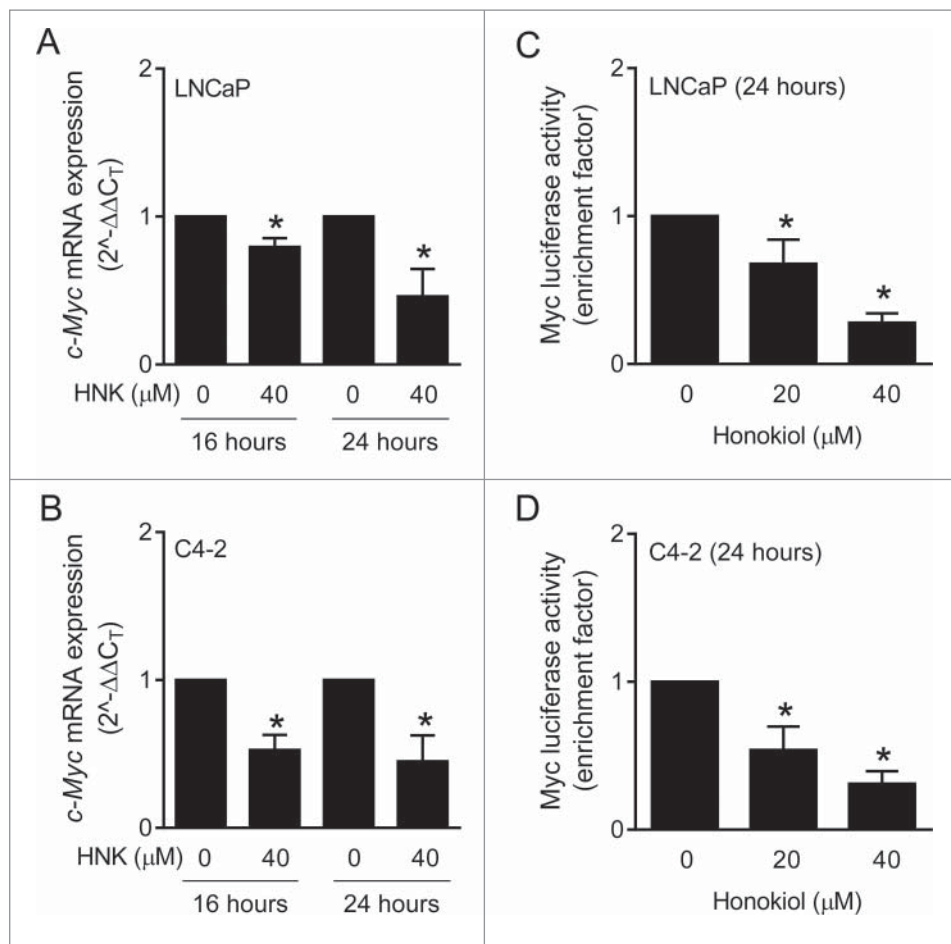


**Figure 4.** HNK treatment decreases *c-Myc* mRNA level and its transcriptional activity in human prostate cancer cells. Real-time PCR for *c-Myc* mRNA in LNCaP (A) and C4-2 (B) cells treated with DMSO or HNK. Relative luciferase activity in LNCaP (C) and C4-2 (D) cells after 24 hour treatment with DMSO or the indicated doses of HNK. Combined results from 2 independent experiments are shown as mean  $\pm$  SD ( $n = 6$ ). Statistical significance compared with DMSO-treated control was analyzed by unpaired Student's *t* test (A and B) or by one-way ANOVA with Dunnett's adjustment (C and D). \*,  $P < 0.05$ .

suppression of *c-Myc* protein level after HNK treatment was shown previously in other cancer cell types,<sup>39-41</sup> but the present study is the first to provide evidence for attenuation of anticancer activity of HNK after *c-Myc* overexpression. We also found that HNK has the ability to downregulate *c-Myc* protein level *in vivo*, although verification of this observation requires further analysis with a larger sample size.

Regulation of *c-Myc* expression is complex and controlled at multiple levels including post-translational modifications.<sup>29</sup> The present study reveals that HNK downregulates *c-Myc* protein level, at least in part by suppressing its transcription. The upstream molecule regulator in *c-Myc* downregulation by HNK is unclear, and requires further investigation. For example, our own work has revealed HNK-mediated inhibition of E2F1, which is one of the transcription factors involved in *c-Myc* regulation.<sup>23,42</sup> Nuclear factor  $\kappa$ B is another pathway implicated in *c-Myc* regulation and HNK treatment inhibits this transcription factor.<sup>39</sup> Additional work is necessary to dissect the role of these pathways in *c-Myc* downregulation by HNK. On the other hand, we are not certain if *c-Myc* downregulation by HNK involves a post-translational mechanism as its effect on *c-Myc* phosphorylation was cell line-specific.

The *c-Myc* regulates many cellular processes including cell cycle progression.<sup>29</sup> For example, *c-Myc* is known to govern

transition of cells from  $G_1$  to S phase.<sup>31</sup> Literature also indicates that loss of *c-Myc* increases  $G_1$  arrest<sup>43</sup> and gain of *c-Myc* triggers exit from  $G_1$  arrest following ionizing radiation.<sup>44</sup> We have previously shown that HNK-induced  $G_1$  phase cell cycle arrest in prostate cancer cells is accompanied by Cyclin D1 downregulation<sup>23</sup> and this effect is attenuated by overexpression of *c-Myc* (present study). Therefore, it is reasonable to conclude that HNK-mediated  $G_1$  arrest in prostate cancer is mediated by inhibition of *c-Myc*.

Exposure of prostate cancer cells to HNK resulted in the reduction of EZH2 protein (present study). The EZH2 protein has recently been implicated in prostate carcinogenesis and metastasis.<sup>32,45</sup> Gene expression profiling revealed that EZH2 is overexpressed in hormone-refractory and metastatic prostate cancer.<sup>45</sup> Moreover, overexpression of EZH2 in prostate cells results in transcriptional repression of a specific cohort of genes.<sup>45</sup> This study also suggested that dysregulated EZH2 expression may distinguish indolent and lethal prostate cancers.<sup>45</sup> *Myc* is also shown to enforce overexpression of EZH2 in early prostatic neoplasia *via* transcriptional and post-transcriptional mechanisms.<sup>32</sup> Another study suggested that *c-Myc* and EZH2 expression together with cell cycle inhibitor p27 may be a prognostic parameter for intermediate-risk prostate cancer patients after the surgery.<sup>46</sup> Because EZH2 knockdown further



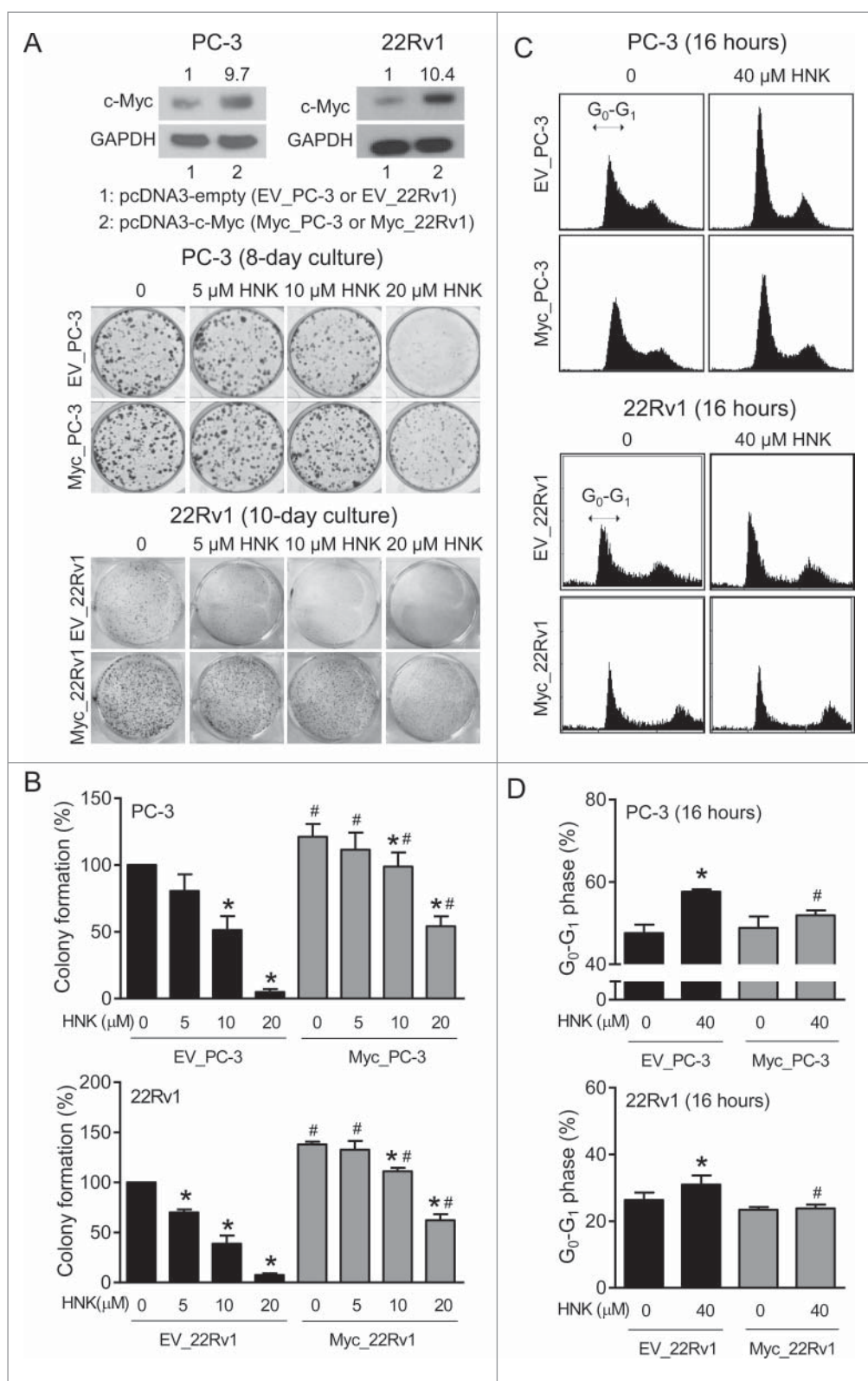


**Figure 5.** Overexpression of c-Myc rescues cell growth inhibition by HNK in prostate cancer cells. (A) *Upper panel*, western blots for c-Myc and loading control GAPDH using lysates from EV\_PC-3, Myc\_PC-3, EV\_22Rv1, and Myc\_22Rv1 cells. *Lower panel*, representative images of colonies from EV\_PC-3, Myc\_PC-3, EV\_22Rv1, and Myc\_22Rv1 cells after treatment with DMSO or the indicated doses of HNK. (B) Quantitation of colony formation. Results are shown as mean  $\pm$  SD (n = 3). Statistically significant compared with respective DMSO-treated control (\*) or between groups at the same treatment (#) by one-way ANOVA with Newman-Keuls multiple comparisons test ( $P < 0.05$ ). Similar results were obtained in independent experiments. (C) Representative cell cycle histograms for EV\_PC-3, Myc\_PC-3, EV\_22Rv1, and Myc\_22Rv1 cells after 16 hour treatment with DMSO or 40  $\mu$ M HNK. (D) Quantitation of G<sub>0</sub>-G<sub>1</sub> phase cells in EV\_PC-3, Myc\_PC-3, EV\_22Rv1, and Myc\_22Rv1 cells. Results are shown as mean  $\pm$  SD (n = 3). Statistically significant compared with respective DMSO-treated control (\*) or between groups at the same treatment (#) by one-way ANOVA with Newman-Keuls multiple comparisons test ( $P < 0.05$ ). Similar results were obtained in independent experiments.

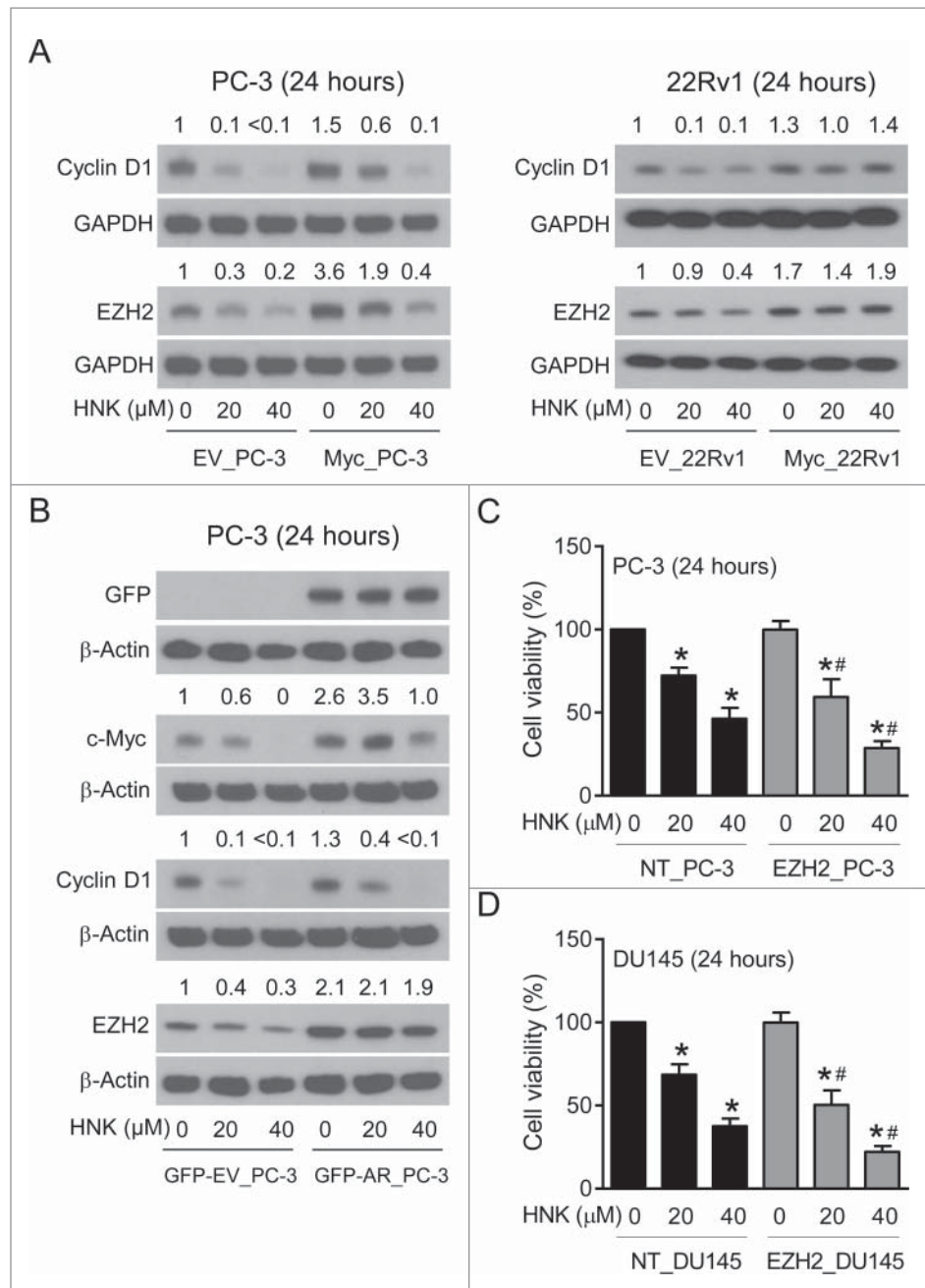


**Figure 6.** Effect of AR overexpression on c-Myc downregulation by HNK. (A) Western blots for Cyclin D1, EZH2, and GAPDH in EV\_PC-3, Myc\_PC-3, EV\_22Rv1, and Myc\_22Rv1 cells after 24 hour treatment with DMSO or the indicated doses of HNK. Numbers on top of bands are fold changes in levels relative to DMSO-treated EV\_PC-3 or EV\_22Rv1 cells. (B) Western blots for GFP, c-Myc, Cyclin D1, EZH2, and  $\beta$ -Actin in GFP-EV\_PC-3 or GFP-AR\_PC-3 cells after 24 hour treatment with DMSO or the indicated doses of HNK. Numbers on top of bands are fold changes in levels relative to DMSO-treated GFP-EV\_PC-3 cells. Effect of stable knockdown of EZH2 on cell viability inhibition by HNK in PC-3 (C) and DU145 (D) cells and their corresponding controls. Results shown are mean  $\pm$  SD (n = 6). Statistically significant compared with respective DMSO-treated control (\*) or between groups at the same treatment (#) by one-way ANOVA with Newman-Keuls multiple comparisons test ( $P < 0.05$ ).

sensitizes prostate cancer cells to growth inhibition by HNK, it is reasonable to postulate that HNK-mediated downregulation of EZH2 is an important contributor to the anticancer effect of HNK.

Safety of HNK has been demonstrated in rodents. For example, thrice every week oral administration of HNK at 50–150 mg/kg body weight for over 100 days was well-tolerated by PC-3 xenograft-bearing male nude mice.<sup>22</sup> HNK was also shown to be safe even after daily treatment at approximately 100 mg/kg body weight via the intraperitoneal route for 6 weeks.<sup>12</sup> While pharmacokinetic behavior of HNK in humans is

yet to be studied, the concentrations used for cellular experiments in the present study were within the plasma achievable range in rats after a single intravenous administration at 20 mg/kg dose.<sup>14</sup>

Because c-Myc overexpression/amplification is observed in a subset of prostate cancer patients,<sup>28,34,36</sup> the present study suggests that HNK may be useful for prevention and/or treatment of the disease. The next step in clinical translation of our cellular findings is to test the *in vivo* efficacy of HNK using transgenic mouse models of c-Myc-driven prostate cancer (e.g., Hi-Myc mouse model). It is equally important to determine if



HNK treatment causes downregulation of *c-Myc* *in vivo*. We did observe a decrease in nuclear *c-Myc* protein level after HNK treatment in the PC-3 xenograft model, but a similar but appropriately powered study is needed to verify this effect in the transgenic mouse model.

In conclusion, the present study reveals that *c-Myc* protein is susceptible to downregulation by HNK treatment in androgen-responsive and androgen-independent human prostate cancer cells. We also provide evidence for a critical role for *c-Myc* in prostate cancer cell growth inhibition by HNK.

## Materials and methods

### Reagents

HNK (98.5%) was purchased from the LKT laboratories (St. Paul, MN) and dissolved in DMSO to make a 50 mM stock solution that was aliquoted and stored at  $-80^{\circ}\text{C}$  until use. Fetal bovine serum (FBS), phosphate-buffered saline (PBS), antibiotic mixture, and F-12K Nutrient Mixture were purchased from Life Technologies-Thermo Fisher Scientific. RPMI1640 and Dulbecco's Modified Eagles Medium were purchased from Mediatech. Anti-*c-Myc* (#5605) antibody used for western blot analysis and immunocytochemistry was from Cell Signaling and anti-EZH2 antibody (#612666) was from BD Biosciences. Antibodies against phospho-(T58)-*c-Myc* (sc-135647), GFP (sc-9996), *c-Myc* (sc-40, for immunohistochemistry), and Cyclin D1 (sc-753) were from Santa Cruz Biotechnology. An antibody specific for detection of phospho-(S62)-*c-Myc* (MAB6763) was from Abnova. The antibody against glyceraldehyde 3-phosphate dehydrogenase (GAPDH, GTX627408) was from GeneTex; and anti- $\alpha$ -tubulin (T5168) and anti- $\beta$ -actin (A5441) antibodies were from Sigma-Aldrich. Alexa-Fluor 488-conjugated rabbit antibody (A11008) was from Life Technologies. G418 (sc-29065B) was from Santa Cruz Biotechnology. Bovine serum albumin (BSA, A7906), 4',6-diamidino-2-phenylindole (DAPI, D9542), and propidium iodide (PI, P4170) were from Sigma-Aldrich.

### Cell lines

PC-3, LNCaP, and 22Rv1 cells were obtained from the American Type Culture Collection and authenticated by us. C4-2 cell line was obtained from UroCor. Mouse prostate cancer cell line *Myc*-CaP was a generous gift from Dr. Charles L. Sawyers (Howard Hughes Medical Institute, Memorial Sloan Kettering Cancer Center, New York, NY). The cells were cultured as recommended by the supplier. PC-3 and 22Rv1 cells were stably transfected with empty pcDNA3 vector (Promega) or *c-Myc* plasmid (Addgene, #16011) in the same vector and selected by G418 treatment. These cells were maintained in medium supplemented with 10% FBS, antibiotic mixture, and 400 (22Rv1) or 800  $\mu\text{g}/\text{mL}$  of G418 (PC-3). VCaP and GFP-AR-overexpressing PC-3 cells were generously provided by Dr. Zhou Wang (University of Pittsburgh, Pittsburgh, PA). VCaP cells were maintained in Dulbecco's Modified Eagles Medium supplemented with 10% FBS and antibiotic mixture. GFP-AR\_PC-3 cells were maintained in RPMI1640 supplemented with 10% FBS, antibiotic mixture, sodium pyruvate, HEPES, 2.5 g/L of

glucose, and 600  $\mu\text{g}/\text{mL}$  of G418. PC-3 and DU145 cells with stable knockdown of EZH2 were a generous gift from Dr. Jeong-Ho Kim (George Washington University, Washington DC), and maintained as recommended by the provider.<sup>47</sup>

### Cell viability assay

Trypan blue dye exclusion assay was performed to assess the effect of HNK on viability of prostate cancer cells including 22Rv1, VCaP, and EZH2 knockdown PC-3 and DU145 cells (designated as EZH2\_PC-3 and EZH2\_DU145, respectively) and their corresponding control cells (designated as NT\_PC-3 and NT\_DU145, respectively) as described by us previously.<sup>48</sup>

### Western blot analysis

Cells were treated with DMSO or desired doses of HNK, lysed, and subjected to sodium dodecyl sulfate-polyacrylamide gel electrophoresis. Immunoblotting was performed as described by us previously.<sup>49</sup> Immunoreactive bands were visualized using chemiluminescence method.

### Immunocytochemistry and immunohistochemistry

Cells were plated on coverslips in 24-well plates. After overnight incubation to allow attachment of the cells, they were treated with DMSO or desired doses of HNK for 24 hours and then fixed and permeabilized with 2% paraformaldehyde and 0.5% Triton X-100, respectively. After blocking with BSA buffer (0.5% BSA and 0.15% glycine in PBS), cells were incubated with *c-Myc* antibody (1:2000 dilution in BSA buffer) overnight at  $4^{\circ}\text{C}$ . Cells were then treated with AlexaFluor 488-conjugated rabbit antibody (1:2000 dilution in BSA buffer) for 1 hour at room temperature in the dark. Cells were stained with DAPI (50 ng/mL) at room temperature in the dark and then mounted. At least 5 non-overlapping images were captured at  $100\times$  objective magnification. *c-Myc* immunohistochemistry was done using archived tumor sections from our previous PC-3 xenograft study.<sup>22</sup> At least 5 non-overlapping images were captured at  $400\times$  magnification and analyzed by Aperio ImageScope software using nuclear algorithm. This software automatically computes blue-negative and red-orange-yellow-positive pixels and categorizes them according to positivity and intensity scale of weak positive, positive, and strong positive. The results are expressed as H-score.

### Quantitative real-time polymerase chain reaction (PCR)

Cells were plated into 6-cm culture dishes, allowed to attach to the plates by overnight incubation, and then treated with DMSO or desired doses of HNK. Total RNA was extracted using RNeasy mini kit from Qiagen. cDNA was synthesized and reverse transcribed using oligo (dT)<sub>20</sub> primer, 1  $\mu\text{g}$  of RNA, and SuperScript<sup>TM</sup> III reverse transcriptase. Real-time PCR was done from 1:10 diluted cDNA using DyNamo HS SYBR Green qPCR kits (Thermo Fisher Scientific) on ABI StepOnePlus PCR Systems. Primers for human *c-Myc* and *GAPDH* were as follows. Forward (*c-Myc*): 5'-GCCACGTCTCACACATCAG-3'; Reverse (*c-Myc*): 5'-TGGTGCATTTTCGTTTGTG-3'; Forward (*GAPDH*): 5'-GGACCTGACCTGCC

GTCTAGAA-3'; Reverse (*GAPDH*): 5'-GGTGTCTGCTGTTG AAGTCAGAG-3'. The PCR conditions were as follows: 95°C for 10 min followed by 40 cycles of 95°C for 15 sec, 60°C for 1 min, and 72°C for 30 sec. Relative gene expression was calculated using the  $2^{-\Delta\Delta CT}$  method.<sup>50</sup>

### Luciferase reporter assay

The pBV-Luc wt MBS1-4 plasmid (2  $\mu$ g; Addgene, #16564) and 0.2  $\mu$ g of pCMV-RL plasmid (Promega) were used for transient transfection. DNA/FuGENE6 (1:3 ratio) mixture was added to LNCaP or C4-2 ( $5 \times 10^4$  cells per well in 12-well plate) cell suspension. After 24 hour co-transfection, the cells were treated with DMSO or desired concentrations of HNK for 24 hours. Luciferase activity was determined using a luminometer.

### Colony formation assay

Cells were seeded in 6-well plates in triplicate. After 24 hours, cells were treated with DMSO or desired doses of HNK. Medium containing DMSO or desired doses of HNK was changed every third day. After 8 (PC-3) or 10 days (22Rv1), cells were fixed with 100% methanol for 5 min at room temperature and stained with 0.5% crystal violet solution in 20% methanol for 30 min at room temperature. Colonies of more than 50 cells were counted using GelCount (Oxford Optronix).

### Determination of $G_0$ - $G_1$ population

Cells plated in 6-well plates were allowed to attach by overnight incubation and then treated with DMSO or 40  $\mu$ M of HNK for 16 hours. Cells were fixed with 70% ethanol for overnight at 4°C. After washing with PBS, cells were stained with PI and analyzed by using BD Accuri C6 flow cytometer.

### Statistical analysis

GraphPad Prism (version 6.07) was used for statistical analyses. Statistical significance of difference was determined by unpaired Student's *t* test for binary comparison or one-way analysis of variance (ANOVA) followed by Dunnett's adjustment (dose-response data) or Newman-Keuls test (multiple comparison).

### Abbreviations

ANOVA	analysis of variance
BSA	bovine serum albumin
AR	androgen receptor
DAPI	4',6-diamidino-2-phenylindole
DMSO	dimethyl sulfoxide
EZH2	Enhancer of Zeste Homolog 2
FBS	fetal bovine serum
GAPDH	glyceraldehyde 3-phosphate dehydrogenase
GFP	green fluorescent protein
HNK	honokiol
PBS	phosphate-buffered saline
PI	propidium iodide

### Disclosure of potential conflicts of interest

No potential conflicts of interest were disclosed.

### Funding

This work was supported by the grant RO1 CA101753 awarded by the National Cancer Institute at the National Institutes of Health (S.V. Singh). This research used the Flow Cytometry Facility and the Tissue and Research Pathology Facility supported in part by a grant from the National Cancer Institute at the National Institutes of Health (P30 CA047904).

### Ethics statement

Paraffin-embedded prostate tumor tissues archived from our previous study were employed to evaluate if *c-Myc* expression was modulated by HNK treatment.<sup>22</sup> The use and care of mice was in accordance with the University of Pittsburgh Institutional Animal Care and Use Committee guidelines.

### References

- [1] Siegel RL, Miller KD, Jemal A. Cancer statistics, 2015. *CA Cancer J Clin* 2015; 65:5-29; PMID:25559415; <http://dx.doi.org/10.3322/caac.21254>
- [2] Huncharek M, Muscat J. Genetic characteristics of prostate cancer. *Cancer Epidemiol Biomarkers Prev* 1995; 4:681-7; PMID:8547836
- [3] Gann PH. Risk factors for prostate cancer. *Rev Urol* 2002; 4:S3-10; PMID:16986064
- [4] Bosland MC, Ozten N, Eskra JN, Mahmoud AM. A perspective on prostate carcinogenesis and chemoprevention. *Curr Pharmacol Rep* 2015; 1:258-65; PMID:26442200; <http://dx.doi.org/10.1007/s40495-015-0031-0>
- [5] Li Y, Ahmad A, Kong D, Bao B, Sarkar FH. Recent progress on nutraceutical research in prostate cancer. *Cancer Metastasis Rev* 2014; 33:629-40; PMID:24375392; <http://dx.doi.org/10.1007/s10555-013-9478-9>
- [6] Lee YJ, Lee YM, Lee CK, Jung JK, Han SB, Hong JT. Therapeutic applications of compounds in the Magnolia family. *Pharmacol Ther* 2011; 130:157-76; PMID:21277893; <http://dx.doi.org/10.1016/j.pharmthera.2011.01.010>
- [7] Fried LE, Arbiser JL. Honokiol, a multifunctional antiangiogenic and antitumor agent. *Antioxid Redox Signal* 2009; 11:1139-48; PMID:19203212; <http://dx.doi.org/10.1089/ars.2009.2440>
- [8] Arora S, Singh S, Piazza GA, Contreras CM, Panyam J, Singh AP. Honokiol: a novel natural agent for cancer prevention and therapy. *Curr Mol Med* 2012; 12:1244-52; PMID:22834827; <http://dx.doi.org/10.2174/156652412803833508>
- [9] Hirano T, Gotoh M, Oka K. Natural flavonoids and lignans are potent cytostatic agents against human leukemic HL-60 cells. *Life Sci* 1994; 55:1061-9; PMID:8084211; [http://dx.doi.org/10.1016/0024-3205\(94\)00641-5](http://dx.doi.org/10.1016/0024-3205(94)00641-5)
- [10] Bai X, Cerimele F, Ushio-Fukai M, Waqas M, Campbell PM, Govindarajan B, Der CJ, Battle T, Frank DA, Ye K, et al. Honokiol, a small molecular weight natural product, inhibits angiogenesis in vitro and tumor growth in vivo. *J Biol Chem* 2003; 278:35501-7; PMID:12816951; <http://dx.doi.org/10.1074/jbc.M302967200>
- [11] Chen F, Wang T, Wu YF, Gu Y, Xu XL, Zheng S, Hu X. Honokiol: a potent chemotherapy candidate for human colorectal carcinoma. *World J Gastroenterol* 2004; 10:3459-63; PMID:15526365; <http://dx.doi.org/10.3748/wjg.v10.i23.3459>
- [12] Shigemura K, Arbiser JL, Sun SY, Zayzafoon M, Johnstone PA, Fujisawa M, Gotoh A, Weksler B, Zhau HE, Chung LW. Honokiol, a natural plant product, inhibits the bone metastatic growth of human prostate cancer cells. *Cancer* 2007; 109:1279-89; PMID:17326044; <http://dx.doi.org/10.1002/cncr.22551>
- [13] Wolf I, O'Kelly J, Wakimoto N, Nguyen A, Amblard F, Karlan BY, Arbiser JL, Koeffler HP. Honokiol, a natural biphenyl, inhibits in

- vitro and in vivo growth of breast cancer through induction of apoptosis and cell cycle arrest. *Int J Oncol* 2007; 30:1529-37; PMID:17487375
- [14] Wang X, Duan X, Yang G, Zhang X, Deng L, Zheng H, Deng C, Wen J, Wang N, Peng C, et al. Honokiol crosses BBB and BCSFB, and inhibits brain tumor growth in rat 9L intracerebral gliosarcoma model and human U251 xenograft glioma model. *PLoS One* 2011; 6:e18490; PMID:21559510; <http://dx.doi.org/10.1371/journal.pone.0018490>
- [15] Wen J, Fu AF, Chen LJ, Xie XJ, Yang GL, Chen XC, Wang YS, Li J, Chen P, Tang MH, et al. Liposomal honokiol inhibits VEGF-D-induced lymphangiogenesis and metastasis in xenograft tumor model. *Int J Cancer* 2009; 124:2709-18; PMID:19219913; <http://dx.doi.org/10.1002/ijc.24244>
- [16] Pan HC, Lai DW, Lan KH, Shen CC, Wu SM, Chiu CS, Wang KB, Sheu ML. Honokiol thwarts gastric tumor growth and peritoneal dissemination by inhibiting Tpl2 in an orthotopic model. *Carcinogenesis* 2013; 34:2568-79; PMID:23828905; <http://dx.doi.org/10.1093/carcin/bgt243>
- [17] Chilampalli S, Zhang X, Fahmy H, Kaushik RS, Zeman D, Hildreth MB, Dwivedi C. Chemopreventive effects of honokiol on UVB-induced skin cancer development. *Anticancer Res* 2010; 30:777-83; PMID:20392996
- [18] Pan J, Zhang Q, Liu Q, Komar SM, Kalyanaraman B, Lubet RA, Wang Y, You M. Honokiol inhibits lung tumorigenesis through inhibition of mitochondrial function. *Cancer Prev Res (Phila)* 2014; 7:1149-59; PMID:25245764; <http://dx.doi.org/10.1158/1940-6207.CAPR-14-0091>
- [19] Li W, Wang Q, Su Q, Ma D, An C, Ma L, Liang H. Honokiol suppresses renal cancer cells' metastasis via dual-blocking epithelial-mesenchymal transition and cancer stem cell properties through modulating miR-141/ZEB2 signaling. *Mol Cells* 2014; 37:383-8; PMID:24810210; <http://dx.doi.org/10.14348/molcells.2014.0009>
- [20] Ponnuram S, Mammen JM, Ramalingam S, He Z, Zhang Y, Umar S, Subramaniam D, Anant S. Honokiol in combination with radiation targets notch signaling to inhibit colon cancer stem cells. *Mol Cancer Ther* 2012; 11:963-72; PMID:22319203; <http://dx.doi.org/10.1158/1535-7163.MCT-11-0999>
- [21] Liu Y, Chen L, He X, Fan L, Yang G, Chen X, Lin X, DU L, Li Z, Ye H, et al. Enhancement of therapeutic effectiveness by combining liposomal honokiol with cisplatin in ovarian carcinoma. *Int J Gynecol Cancer* 2008; 18:652-9; PMID:17892458; <http://dx.doi.org/10.1111/j.1525-1438.2007.01070.x>
- [22] Hahm ER, Arlotti JA, Marynowski SW, Singh SV. Honokiol, a constituent of oriental medicinal herb *Magnolia officinalis*, inhibits growth of PC-3 xenografts in vivo in association with apoptosis induction. *Clin Cancer Res* 2008; 14:1248-57; PMID:18281560; <http://dx.doi.org/10.1158/1078-0432.CCR-07-1926>
- [23] Hahm ER, Singh SV. Honokiol causes G0-G1 phase cell cycle arrest in human prostate cancer cells in association with suppression of retinoblastoma protein level/phosphorylation and inhibition of E2F1 transcriptional activity. *Mol Cancer Ther* 2007; 6:2686-95; PMID:17938262; <http://dx.doi.org/10.1158/1535-7163.MCT-07-0217>
- [24] Hahm ER, Karlsson AI, Bonner MY, Arbiser JL, Singh SV. Honokiol inhibits androgen receptor activity in prostate cancer cells. *Prostate* 2014; 74:408-20; PMID:24338950; <http://dx.doi.org/10.1002/pros.22762>
- [25] Gao L, Schwartzman J, Gibbs A, Lisac R, Kleinschmidt R, Wilmot B, Bottomly D, Coleman I, Nelson P, McWeeney S, et al. Androgen receptor promotes ligand-independent prostate cancer progression through c-Myc upregulation. *PLoS One* 2013; 8:e63563; PMID:23704919; <http://dx.doi.org/10.1371/journal.pone.0063563>
- [26] Tsai TH, Chou CJ, Cheng FC, Chen CF. Pharmacokinetics of honokiol after intravenous administration in rats assessed using high-performance liquid chromatography. *J Chromatogr B Biomed Appl* 1994; 655:41-5; PMID:8061832; [http://dx.doi.org/10.1016/0378-4347\(94\)00031-X](http://dx.doi.org/10.1016/0378-4347(94)00031-X)
- [27] Watson PA, Ellwood-Yen K, King JC, Wongvipat J, Lebeau MM, Sawyers CL. Context-dependent hormone-refractory progression revealed through characterization of a novel murine prostate cancer cell line. *Cancer Res* 2005; 65:11565-71; PMID:16357166; <http://dx.doi.org/10.1158/0008-5472.CAN-05-3441>
- [28] Gurel B, Iwata T, Koh CM, Jenkins RB, Lan F, Van Dang C, Hicks JL, Morgan J, Cornish TC, Sutcliffe S, et al. Nuclear MYC protein overexpression is an early alteration in human prostate carcinogenesis. *Mod Pathol* 2008; 21:1156-67; PMID:18567993; <http://dx.doi.org/10.1038/modpathol.2008.111>
- [29] Sears RC. The life cycle of C-Myc: From synthesis to degradation. *Cell Cycle* 2004; 3:1133-7; PMID:15467447; <http://dx.doi.org/10.4161/cc.3.9.1145>
- [30] Sachdeva M, Zhu S, Wu F, Wu H, Walia V, Kumar S, Elble R, Watabe K, Mo YY. p53 represses c-Myc through induction of the tumor suppressor miR-145. *Proc Natl Acad Sci U S A* 2009; 106:3207-12; PMID:19202062; <http://dx.doi.org/10.1073/pnas.0808042106>
- [31] Bretones G, Delgado MD, León J. Myc and cell cycle control. *Biochim Biophys Acta* 2015; 1849:506-16; PMID:24704206; <http://dx.doi.org/10.1016/j.bbagg.2014.03.013>
- [32] Koh CM, Iwata T, Zheng Q, Bethel C, Yegnasubramanian S, De Marzo AM. Myc enforces overexpression of EZH2 in early prostatic neoplasia via transcriptional and post-transcriptional mechanisms. *Oncotarget* 2011; 2:669-83; PMID:21941025; <http://dx.doi.org/10.18632/oncotarget.327>
- [33] Dang CV. MYC on the path to cancer. *Cell* 2012; 149:22-35; PMID:22464321; <http://dx.doi.org/10.1016/j.cell.2012.03.003>
- [34] Koh CM, Bieberich CJ, Dang CV, Nelson WG, Yegnasubramanian S, De Marzo AM. MYC and prostate cancer. *Genes Cancer* 2010; 1:617-28; PMID:21779461; <http://dx.doi.org/10.1177/1947601910379132>
- [35] Iwata T, Schultz D, Hicks J, Hubbard GK, Mutton LN, Lotan TL, Bethel C, Lotz MT, Yegnasubramanian S, Nelson WG, et al. MYC overexpression induces prostatic intraepithelial neoplasia and loss of Nkx3.1 in mouse luminal epithelial cells. *PLoS One* 2010; 5:e9427; PMID:20195545; <http://dx.doi.org/10.1371/journal.pone.0009427>
- [36] Jenkins RB, Qian J, Lieber MM, Bostwick DG. Detection of c-myc oncogene amplification and chromosomal anomalies in metastatic prostatic carcinoma by fluorescence and chromosomal anomalies in situ hybridization. *Cancer Res* 1997; 57:524-31; PMID:9012485
- [37] Zhang X, Lee C, Ng P-Y, Rubin M, Shabsigh A, Buttyan R. Prostatic neoplasia in transgenic mice with prostate-directed overexpression of c-myc oncoprotein. *Prostate* 2000; 43:278-85; PMID:10861747; [http://dx.doi.org/10.1002/1097-0045\(20000601\)43:4%3c278::AID-PROS7%3e3.0.CO;2-4](http://dx.doi.org/10.1002/1097-0045(20000601)43:4%3c278::AID-PROS7%3e3.0.CO;2-4)
- [38] Ellwood-Yen K, Graeber TG, Wongvipat J, Iruela-Arispe ML, Zhang J, Matusik R, Thomas GV, Sawyers CL. Myc-driven murine prostate cancer shares molecular features with human prostate tumors. *Cancer Cell* 2003; 4:223-38; PMID:14522256; [http://dx.doi.org/10.1016/S1535-6108\(03\)00197-1](http://dx.doi.org/10.1016/S1535-6108(03)00197-1)
- [39] Ahn KS, Sethi G, Shishodia S, Sung B, Arbiser JL, Aggarwal BB. Honokiol potentiates apoptosis, suppresses osteoclastogenesis, and inhibits invasion through modulation of nuclear factor- $\kappa$ B activation pathway. *Mol Cancer Res* 2006; 4:621-33; PMID:16966432; <http://dx.doi.org/10.1158/1541-7786.MCR-06-0076>
- [40] Park EJ, Min HY, Chung HJ, Hong JY, Kang YJ, Hung TM, Youn UJ, Kim YS, Bae K, Kang SS, et al. Down-regulation of c-Src/EGFR-mediated signaling activation is involved in the honokiol-induced cell cycle arrest and apoptosis in MDA-MB-231 human breast cancer cells. *Cancer Lett* 2009; 277:133-40; PMID:19135778; <http://dx.doi.org/10.1016/j.canlet.2008.11.029>
- [41] Yao CJ, Lai GM, Yeh CT, Lai MT, Shih PH, Chao WJ, Whang-Peng J, Chuang SE, Lai TY. Honokiol eliminates human oral cancer stem-like cells accompanied with suppression of Wnt/ $\beta$ -Catenin signaling and apoptosis induction. *Evid Based Complement Alternat Med* 2013; 2013:146136; PMID:23662112
- [42] Oswald F, Lovéc H, Mörröy T, Lipp M. E2F-dependent regulation of human MYC: trans-activation by cyclins D1 and A overrides tumour suppressor protein functions. *Oncogene* 1994; 9:2029-36; PMID:8208548
- [43] Schorl C, Sedivy JM. Loss of protooncogene c-Myc function impedes G1 phase progression both before and after the restriction point. *Mol Biol Cell* 2003; 14:823-35; PMID:12631706; <http://dx.doi.org/10.1091/mbc.E02-10-0649>



- [44] Sheen JH, Dickson RB. Overexpression of c-Myc alters G<sub>1</sub>/S arrest following ionizing radiation. *Mol Cell Biol* 2002; 22:1819-33; PMID:11865060; <http://dx.doi.org/10.1128/MCB.22.6.1819-1833.2002>
- [45] Varambally S, Dhanasekaran SM, Zhou M, Barrette TR, Kumar-Sinha C, Sanda MG, Ghosh D, Pienta KJ, Sewalt RG, Otte AP, et al. The polycomb group protein EZH2 is involved in progression of prostate cancer. *Nature* 2002; 419:624-9; PMID:12374981; <http://dx.doi.org/10.1038/nature01075>
- [46] Li K, Chen MK, Situ J, Huang WT, Su ZL, He D, Gao X. Role of co-expression of c-Myc, EZH2 and p27 in prognosis of prostate cancer patients after surgery. *Chin Med J* 2013; 126:82-7; PMID:23286483
- [47] Shin YJ, Kim JH. The role of EZH2 in the regulation of the activity of matrix metalloproteinases in prostate cancer cells. *PLoS One* 2012; 7:e30393; PMID:22272343; <http://dx.doi.org/10.1371/journal.pone.0030393>
- [48] Xiao D, Choi S, Johnson DE, Vogel VG, Johnson CS, Trump DL, Lee YJ, Singh SV. Diallyl trisulfide-induced apoptosis in human prostate cancer cells involves c-Jun N-terminal kinase and extracellular-signal regulated kinase-mediated phosphorylation of Bcl-2. *Oncogene* 2004; 23:5594-606; PMID:15184882; <http://dx.doi.org/10.1038/sj.onc.1207747>
- [49] Xiao D, Srivastava SK, Lew KL, Zeng Y, Hershberger P, Johnson CS, Trump DL, Singh SV. Allyl isothiocyanate, a constituent of cruciferous vegetables, inhibits proliferation of human prostate cancer cells by causing G<sub>2</sub>/M arrest and inducing apoptosis. *Carcinogenesis* 2003; 24:891-7; PMID:12771033; <http://dx.doi.org/10.1093/carcin/bgg023>
- [50] Livak KJ, Schmittgen TD. Analysis of relative gene expression data using real-time quantitative PCR and the 2<sup>-ΔΔCT</sup> Method. *Methods* 2001; 25:402-8; PMID:11846609; <http://dx.doi.org/10.1006/meth.2001.1262>